

Published in final edited form as:

J Am Coll Cardiol. 2011 November 22; 58(22): 2332–2339. doi:10.1016/j.jacc.2011.07.048.

Inhibition of c-Src Tyrosine Kinase Prevents Angiotensin II-Mediated Connexin43 Remodeling and Sudden Cardiac Death

Ali A. Sovari, MD¹, Shahriar Iravanian, MD², Elena Dolmatova, MD³, Zhe Jiao, MD, PhD², Hong Liu, MD, PhD¹, Shadi Zandieh, MD¹, Vibhash Kumar, MD¹, Kun Wang, MD¹, Kenneth E. Bernstein, MD⁴, Marcelo G. Bonini, PhD¹, Heather Duffy, PhD³, and Samuel C. Dudley, MD, PhD, FACC¹

¹ Section of Cardiology and Center for Cardiovascular Research, University of Illinois at Chicago, Illinois 60612

² Section of Cardiology, Emory University, Atlanta, Georgia 30033

³ Section of Cardiology, Beth Israel Deaconess Medical Center, Harvard Medical School, Boston, Massachusetts 02115

⁴ Departments of Pathology and Biomedical Sciences, Cedars-Sinai Medical Center, Los Angeles, California 90048

Abstract

Objectives—We sought to test whether c-Src tyrosine kinase mediates connexin 43 (Cx43) reduction and sudden cardiac death in a transgenic mouse model of cardiac-restricted overexpression of angiotensin-converting enzyme (ACE8/8).

Background—Renin-angiotensin system (RAS) activation is associated with an increased risk of arrhythmia and sudden cardiac death; however, that mechanism is not well understood. The upregulation of c-Src by angiotensin II may result in the reduction of Cx43, which impairs gap junction function and provides a substrate for arrhythmia.

Method—Wild-type and ACE8/8 mice with and without treatment with the c-Src inhibitor PP1 were studied. Telemetry monitoring, in vivo electrophysiology studies, Western blot analyses for total and phosphorylated c-Src and Cx43, immunohistochemistry staining for Cx43, and functional assessment of Cx43 with fluorescent dye diffusion were performed.

Results—The majority of the arrhythmic deaths resulted from ventricular tachycardia degenerating to ventricular fibrillation (83%). Levels of total and phosphorylated c-Src were increased and Cx43 reduced in ACE8/8 mice. PP1 reduced total and phospho c-Src levels, increased the Cx43 level by 2.1-fold ($P < 0.005$), increased Cx43 at the gap junctions (immunostaining), improved gap junctional communication (dye spread), and reduced ventricular tachycardia inducibility and sudden cardiac death. The survival rate increased from 11% to 86% with four weeks of PP1 treatment ($P < 0.005$). Treatment with an inactive analog did not change survival or Cx43 levels.

© 2011 American College of Cardiology Foundation. Published by Elsevier Inc. All rights reserved.

Corresponding author: Dr. Samuel C. Dudley, Jr Section of Cardiology, University of Illinois at Chicago 840 S. Wood Street, MC 715 Chicago, IL 60612 Phone: (312) 996-9096 Fax: (312) 413-2948 scdudley@uic.edu.

Publisher's Disclaimer: This is a PDF file of an unedited manuscript that has been accepted for publication. As a service to our customers we are providing this early version of the manuscript. The manuscript will undergo copyediting, typesetting, and review of the resulting proof before it is published in its final citable form. Please note that during the production process errors may be discovered which could affect the content, and all legal disclaimers that apply to the journal pertain.

Conclusion—RAS activation is associated with c-Src upregulation, Cx43 loss, reduced myocyte coupling, and arrhythmic sudden death, which can be prevented by c-Src inhibition. This suggests that an increase in c-Src activity may help mediate RAS-induced arrhythmias and that c-Src inhibitors might exert antiarrhythmic activity.

Keywords

Angiotensin II; c-Src tyrosine kinase; connexin43; sudden cardiac death

Introduction

The renin-angiotensin system (RAS) is a key signaling pathway, and the activation of that system is associated with an increased incidence of cardiovascular death (1;2). In humans, increased angiotensin II (Ang II) levels are associated with an increased risk of ventricular arrhythmia (3), and treatment with an angiotensin-converting enzyme (ACE) inhibitor reduces that risk (4-8). Nevertheless, it is not completely understood how RAS system activation increases arrhythmic risk.

A critical component of the RAS system is the ACE, which cleaves the decapeptide angiotensin I to produce the 8 amino acid peptide Ang II, a central signaling molecule of the RAS system. Previously, we developed a transgenic mouse model of RAS activation by overexpression of ACE restricted to the heart (ACE8/8 mice) via replacement of the somatic ACE promoter with the cardiac-specific α -myosin heavy chain promoter (9). These mice (ACE8/8) are not hypertensive, have structurally normal left ventricle with a normal left ventricular ejection fraction (LVEF), and have no ventricular fibrosis. They exhibit cardiac oxidative stress, a high incidence of ventricular tachycardia and ventricular fibrillation (VT/VF), and subsequent sudden cardiac death (SCD) associated with reduced ventricular connexin 43 (Cx43) levels (10). Treatment with ACE inhibitor and Ang II receptor 1 blocker reduce the arrhythmic risk and increase the Cx43 level (11). In the adult heart, ventricular gap junctions are formed primarily by Cx43 protein. A significant reduction in or lack of Cx43 can result in slow conduction velocity and ventricular arrhythmia (12). The molecular mechanism by which RAS activation causes the decrease in Cx43 is unknown, however.

The tyrosine kinase c-Src has been linked primarily to tumor growth, and the inhibition of c-Src has been shown to be effective in controlling cancers (13-17). We have shown that in an animal model of myocardial infarction, the upregulation of c-Src and an increase in the level of phosphorylated Tyr 416 c-Src (the active form of c-Src) result in the downregulation of Cx43 by competition between phosphorylated c-Src and Cx43 for a binding site at zonula occludens-1, an intercalated disk scaffolding protein (18). Elevated levels of reactive oxygen species and Ang II can result in the upregulation of c-Src (19-21). We postulated that a cause of Cx43 reduction and sudden death in ACE8/8 mice was an increased level of c-Src and that the inhibition of c-Src would increase Cx43 and improve survival in ACE8/8 mice.

Materials and Methods

The derivation and electrophysiological characterization of ACE8/8 mice have been described previously (9;10), and it has been shown by telemetry monitoring that the cause of SCD in those animals are VT/VF, asystole and slowed conduction (10). We repeated telemetry monitoring for wild-type and ACE8/8 mice in this study. Wild-type mice with and without treatment with the c-Src inhibitor 1-(1,1-dimethylethyl)-1-(4-methylphenyl)-1H-pyrazolo[3, 4-d]pyrimidin-4-amine (PP1), ACE8/8 mice with and without treatment with PP1, and ACE8/8 mice treated with 1-phenyl-1H-pyrazolo[3,4-d]pyrimidin-4-amine (PP3), an inactive analog of PP1, were studied. The animal experiments were conducted according

to the National Institutes of Health (NIH) Guide for the Care and Use of Experimental Animals and were approved by the University of Illinois Institutional Animal Care and Use Committee. Mice of both sexes were treated with 1.5-mg/kg PP1 (Enzo Life Sciences, Plymouth Meeting, PA), a specific inhibitor of c-Src tyrosine kinase, twice weekly for 4 consecutive weeks by intraperitoneal injection (22-24). PP3 (Enzo Life Sciences) was administered intraperitoneally at the same dose (1.5 mg/kg twice weekly for 4 consecutive weeks). The treatment of all animals was initiated when the mice were 30 days old.

Telemetry Monitoring and Electrophysiology Study

Seven ACE 8/8 mice of 5 weeks old, and six C57BL/6 control mice, were implanted with ETAF10 transmitters (Data Sciences International, St. Paul, M.N.). Briefly, mice were anesthetized by intraperitoneal injection of ketamine (100 mg/kg) and xylazine (10 mg/kg) cocktail. A skin incision was made at right abdominal region and a transmitter was inserted subcutaneously to the left. The two electrocardiogram (ECG) leads were tunneled and positioned under skin to generate a lead II electrocardiographic configuration. The skin incision was then closed and the animals were followed by telemetry for a maximum of 3 weeks or until their death. Twenty four hours after transmitter implantation, ECG signals recorded between 12 to 3 pm, when mice were relatively calm and resting, were used to calculate baseline heart rate. The ECG signals immediately prior to the death were analyzed for rhythm changes. The heart rate calculation and cardiac rhythm analysis were performed using Dataquest ART Version 4.1 software (DSI).

For the electrophysiology studies, the mice were anesthetized with an intraperitoneal injection of ketamine (100 mg/kg) and xylazine (5 mg/kg). After cutdown, a 1.1-F catheter with 0.5-mm interelectrode spacing (EPR 800, Millar Instruments, Houston, TX) was placed into the right jugular vein and was advanced into the right ventricle. A constant current stimulator (A320, World Precision Instruments, Sarasota, FL) connected to a laptop computer was used for cardiac stimulation. During the experiment, body temperature was maintained at 37°C with a warming pad. Burst pacing at cycle lengths of 100 to 50 ms was used to test for VT inducibility. A rhythm with more than 3 consecutive ventricular beats was considered to be VT.

Western blot analysis

The mice were killed, and their hearts were excised. The ventricular tissue was homogenized in a buffer containing 20 mM of tris-(hydroxymethyl)-aminomethane (Tris-Cl) (pH, 7.4), 150 mM of sodium chloride (NaCl), 2.5 mM of ethylenediamine tetraacetic acid (EDTA), 1% Triton-100, 10 µL/mL of phenylmethylsulfonyl fluoride (PMSF), 10 µL/mL of protein inhibitor cocktail (Pierce, Rockford, IL), and 10 µL/mL of phosphatase inhibitor cocktail II (Sigma-Aldrich, St. Louis, MO). Protein samples (5 to 20 µg) were separated via 10% sodium dodecyl sulfate polyacrylamide gel electrophoresis (SDS-PAGE) and were transferred to nitrocellulosemembranes. The membranes were blotted with the primary antibodies against c-Src, phosphorylated (Tyr 416) c-Src, and Cx43 (Cell Signaling, Danvers, MA) and ACE (Millipore, Temecula, CA). For a loading control, the membranes were blotted with a primary antibody against glyceraldehyde-3-phosphate dehydrogenase (GAPDH; Santa Cruz Biotech, Santa Cruz, CA). After treatment with secondary antirabbit or antimouse antibodies, imaging was performed with enhanced chemiluminescence. The radiographic film images were scanned and analyzed with NIH ImageJ software.

Immunohistochemistry

The mouse hearts were fixed in 10% formalin, after which 8-µm thick sections were blocked for 1 hour at room temperature and were then incubated with anti-Cx43 antibodies overnight

at 4°C at concentrations known to provide the best signal-to-noise ratio. The slides were reviewed with a Zeiss Axioskop microscope (Carl Zeiss, Inc, Thornwood, NY), and photomicrographs with original magnification $\times 40$ were taken from the apex, the mid-left ventricle (LV), and the LV base. From each of those sites, photomicrographs were taken from the endocardium and epicardium. The Cx43 content was quantified with the use of a grid that divided the field of view into 200 squares. At the intersection points aligning with the intercalated disks, Cx43 was scored as “1” (present) or “0” (absent). The results were expressed as the percentage occupied by Cx43 in the total area examined, excluding pseudospaces. This method has been used previously to quantify levels of collagen and Cx43 in cardiac tissue (25;26).

Functional assessment of Cx43

We used an established technique for measuring Cx43 function that involves fluorescent dye introduction and diffusion in intact heart muscle (27). Fresh hearts were obtained from wild-type, ACE8/8, ACE8/8 PP1-treated, and ACE8/8 PP3-treated mice. A sample from each heart was placed in phosphate buffered saline at 37°C, the anterior surface of the LV was punctured with a 27-gauge needle, and the sample was incubated with a droplet of 0.5% Lucifer yellow (LY) and a droplet of 0.5% Texas Red Dextran (TRD) in 150 mM of LiCl solution. After a 15-minute incubation, the samples were fixed in 4% formaldehyde for 30 minutes, washed in phosphate-buffered saline, frozen in liquid nitrogen, and sliced into 14- μ m sections. The sections were mounted on microscope slides and examined on a Leica DM5000 B epifluorescence microscope (Leica Microsystems Inc., Bannockburn, IL). Digital images of the spread of LY and TRD were obtained. The measurement of the dye spread was performed with ImageJ software. Molecules of TRD are too large to traverse gap junctions and stains cells with disrupted membrane. The TRD distribution was subtracted from the length of the LY spread at the same site to measure the true LY spread through gap junctions. Dye spread in longitudinal and transverse directions was assessed.

Statistical analysis

The values are presented as the mean \pm the SEM. The *t* test, one-way analysis of variance with post hoc tests of significance, the Tukey honestly significant test, and the Fisher exact test for 2×2 tables were used where appropriate, and a *P* value of < 0.05 was considered statistically significant. The survival data were analyzed with the Kaplan-Meier method, and the *P* value was calculated with the log-rank test. The correlation was assessed with the Pearson correlation coefficient method.

Results

PP1 treatment prevents SCD and reduces VT inducibility

Baseline heart rate was similar between the control and ACE 8/8 groups (548 ± 17 bpm vs. 491 ± 34 bpm, *P* = NS). All the control mice survived until the end of the telemetry follow-up. In contrast, 6 out of 7 ACE 8/8 mice died within 5-23 days (10 ± 3 days) after transmitter implantation. Rhythm analysis showed one mouse died because of progressive bradycardia and five died because of VT degenerating to VF (Figure 1). Treatment with PP1 significantly improved the survival rate of ACE8/8 mice from 3 of 30 SCD and a mean survival time of 10.2 ± 1.5 days to 20 of 23 and a mean survival time of 24.7 ± 0.2 days during the 30 days of treatment and observation (*P* < 0.005) (Figure 1). The treatment of wild-type mice with PP1 was not associated with any adverse reaction. The treatment of ACE8/8 mice with PP3, the inactive analog, did not result in a statistically significant improvement in the survival rate when compared with untreated ACE 8/8 mice (11.2 ± 1.2 days vs. 10.2 ± 1.5 days, *P* = NS). VT inducibility was observed in 3.3% of the wild-type

mice (n=30) and in 86.9% of the ACE8/8 mice (n = 23; P < 0.005). PP1-treated ACE8/8 mice showed a significant reduction in VT inducibility (86.9% vs. 50%, P < 0.05) (Figure 1).

PP1 treatment reduces c-Src and raises Cx43 levels

Western blot of the total and phosphorylated (Tyr416) forms of c-Src protein showed a 1.5-fold increase in the total c-Src level and a 2.6-fold increase in the level of phospho-Src protein in the hearts of ACE8/8 mice when compared with those levels in control hearts (P < 0.05). In untreated ACE8/8 mice, the level of Cx43 protein was 36% of its level in wild-type mice (P < 0.005) (Figure 2A). In addition, the level of Cx43 was lower in ACE8/8 mice with SCD when compared with those animals that did not experience SCD during the treatment time period (57.8%, P < 0.05). PP1 treatment in ACE8/8 mice reduced the total and the phospho-(Tyr416) c-Src protein levels to 58% and 75%, respectively, of those levels in untreated ACE8/8 mice (P < 0.05) (Figure 2B). PP1 treatment also caused a 2.1-fold increase in the Cx43 protein level in treated ACE8/8 mice compared with untreated ACE8/8 mice (P < 0.005). The correlation between the levels of phospho-(Tyr416) c-Src and Cx43 was statistically significant in ACE8/8 mice (R = -0.85, P < 0.05). Treatment of ACE8/8 mice with inactive PP3 did not increase the total Cx43 protein level (P = NS). Treatment of wild-type control mice with PP1 did not change the total Cx43 level (Figure 2C). Gene microarray analysis did not show any statistically significant change in the messenger RNA abundances of Cx43. Treatment of ACE8/8 mice with PP1 did not decrease the ACE level (Figure 2C).

Immunohistochemical analysis showed that the Cx43 level was significantly lower in the ACE8/8 untreated hearts than in the wild-type hearts ($5.4 \pm 0.7\%$ vs. $18.3 \pm 0.6\%$, P < 0.005) (Figure 3). PP1 treatment caused a 2.0-fold increase in the Cx43 content in the ACE8/8 mouse hearts (P < 0.005). The extent of that improvement in the Cx43 level after PP1 treatment was consistent with the 2.1-fold increase in the total protein level for Cx43 noted on Western blot analysis. The immunostaining for Cx43 showed that the Cx43 level was increased at intercalated disks. Treatment with the inactive analog PP3 did not increase the Cx43 level at the gap junctions when compared with untreated ACE8/8 mice (P = NS).

c-Src Inhibition improves gap junction function

Analysis of dye spread as a functional measure of Cx43 activity showed that LY migration in ACE 8/8 mice was 66% of that in wild-type mice (0.14 ± 0.01 mm vs. 0.21 ± 0.02 mm respectively, P < 0.05), which indicates reduced gap junction function in ACE8/8 mice (Figure 4). Treatment with the c-Src inhibitor PP1 restored gap junction function to that of wild-type mice (0.14 ± 0.01 mm in ACE8/8 vs. 0.21 ± 0.02 mm in PP1-treated ACE8/8 mice, P < 0.05; wild-type vs. PP1, P = NS). The analysis of dye spread in longitudinal and transverse directions separately showed that the changes in dye spread were more prominent in a longitudinal than in a transverse direction. This is consistent with the immunohistochemical result that Cx43 increased most at the intercalated disks. PP3 had no statistically significant effect on dye diffusion.

Discussion

The telemetry study showed that the mode of SCD in ACE8/8 mice is mainly VT/VF and occasionally severe bradyarrhythmia. This result confirms our previous telemetry recording in these animals (10), and the observed arrhythmias resulting in SCD are consistent with human findings (28). The cardiac sodium channel generates the main current for conduction, but ACE8/8 mice have no significant change in their sodium current; however, their level of Cx43 is dramatically reduced (10). Cx43 is the major protein of ventricular gap junctions

that are low-resistance conduits for electrical conduction in the heart. In this study, we show that c-Src is upregulated in these animals and that it mediates the effect of Ang II in reducing Cx43 and causing VT/VF. That finding is consistent with those of other investigators showing that Ang II and oxidative stress upregulates c-Src (19-21). In addition, treatment with Losartan, an Ang II type 1 receptor blocker, reduces the active form of Src protein in ACE8/8 mice supporting that the observed change in the level of Src is due to the elevated level of Ang II and via the binding to its type 1 receptor (supplement figure). We have previously shown that ACE 8/8 mice show cardiac oxidation, and this might be one mechanism for the increase in activated c-Src.

c-Src can result in the reduction of the Cx43 level via its competition with Cx43 for binding to zonula occludens-1. Increased phospho (Tyr416)-c-Src results in the unbinding of Cx43 from gap junctions, diffusion away from the intercalated disk, and enzymatic degradation (18). This may not be the sole mechanism by which c-Src upregulation results in a reduction in Cx43. Nevertheless, the effect of PP1 on the inhibition of c-Src, the increase in the level of Cx43, and the statistically significant inverse correlation between the levels of phosphorylated c-Src and Cx43 support a cause-effect relationship between the upregulation of c-Src and a reduction in Cx43. Cx43 RNA abundance was unchanged in ACE 8/8 mice and with treatment suggesting that the effects of c-Src and PP1 were post-transcriptional. The increased level of ACE in ACE8/8 mice compared to the control animals did not change with PP1 treatment arguing that the effect of PP1 was downstream of RAS activation.

We showed that improvement in the total Cx43 level occurred primarily at the intercalated disks and was correlated with an improvement in gap junction function measured with dye diffusion. The increase in Cx43 and the increase in the ease of dye spread were associated with a reduced risk of VT inducibility and sudden death. Cx43 reversal was not complete in our study, but the changes noted were in a range consistent with a significant reduction in sudden death. Homozygous Cx43 knockout mice die from ventricular arrhythmia and conduction blocks (12;29). Nevertheless, heterozygote Cx43^{+/-} mice with ~50% of the normal level of Cx43 are not prone to ventricular arrhythmias and cardiac death (29), which suggests that a reduction of more than 50% of the normal level of Cx43 is required for electrical conduction to be significantly impaired and cause arrhythmic death. In our case, c-Src inhibition in ACE8/8 mice increased Cx43 levels from 36% to 68% and was associated with an improvement in survival from 11% to 86% during the 4 weeks of the treatment with PP1. This is consistent with prior data in genetically altered mice and with model predictions that the full restoration of Cx43 levels is not necessary to achieve a significant therapeutic effect (30).

In conclusion, RAS activation is associated with c-Src upregulation, Cx43 loss, reduced myocyte coupling, and arrhythmic sudden death. Those effects can be ameliorated by c-Src inhibition, which suggests that an increase in c-Src activity may participate in RAS-induced arrhythmias and that c-Src inhibitors might exert antiarrhythmic activity in states of RAS activation. Since we used a model of RAS activation limited to the heart, results may vary with in vivo systemic RAS activation.

Supplementary Material

Refer to Web version on PubMed Central for supplementary material.

Acknowledgments

Grants and supports: National Institute of Health RO1 RO1HL085558, P01 HL058000, and American Heart Association Midwest Affiliate Postdoctoral Fellowship # AHA10POST4450037

Abbreviations list

ACE	Angiotensin-converting enzyme
Ang II	Angiotensin II
Cx43	Connexin 43
LY	Lucifer yellow
LV	Left ventricle
LVEF	Left ventricular ejection fraction
RAS	Renin-angiotensin system
SCD	Sudden cardiac death
TRD	Texas Red Dextran
VF	Ventricular fibrillation
VT	Ventricular tachycardia

References

1. Lonn EM, Yusuf S, Jha P, et al. Emerging role of angiotensin-converting enzyme inhibitors in cardiac and vascular protection. *Circulation*. 1994; 90(4):2056–69. [PubMed: 7923694]
2. Pagliaro P, Penna C. Rethinking the renin-angiotensin system and its role in cardiovascular regulation. *Cardiovasc Drugs Ther*. 2005; 19(1):77–87. [PubMed: 15883759]
3. Akar FG, Spragg DD, Tunin RS, Kass DA, Tomaselli GF. Mechanisms underlying conduction slowing and arrhythmogenesis in nonischemic dilated cardiomyopathy. *Circ Res*. 2004; 95(7):717–25. [PubMed: 15345654]
4. Teo KK, Mitchell LB, Pogue J, Bosch J, Dagenais G, Yusuf S. Effect of ramipril in reducing sudden deaths and nonfatal cardiac arrests in high-risk individuals without heart failure or left ventricular dysfunction. *Circulation*. 2004; 110(11):1413–7. [PubMed: 15353497]
5. Kober L, Torp-Pedersen C, Carlsen JE, et al. A clinical trial of the angiotensin-converting-enzyme inhibitor trandolapril in patients with left ventricular dysfunction after myocardial infarction. Trandolapril Cardiac Evaluation (TRACE) Study Group. *N Engl J Med*. 1995; 333(25):1670–6. [PubMed: 7477219]
6. Domanski MJ, Mitchell GF, Norman JE, Exner DV, Pitt B, Pfeffer MA. Independent prognostic information provided by sphygmomanometrically determined pulse pressure and mean arterial pressure in patients with left ventricular dysfunction. *J Am Coll Cardiol*. 1999; 33(4):951–8. [PubMed: 10091821]
7. Yusuf S, Sleight P, Pogue J, Bosch J, Davies R, Dagenais G. Effects of an angiotensin-converting-enzyme inhibitor, ramipril, on cardiovascular events in high-risk patients. The Heart Outcomes Prevention Evaluation Study Investigators. *N Engl J Med*. 2000; 342(3):145–53. [PubMed: 10639539]
8. Hattori Y, Atsushi S, Hiroaki F, Toyama J. Effects of cilazapril on ventricular arrhythmia in patients with congestive heart failure. *Clin Ther*. 1997; 19(3):481–6. [PubMed: 9220212]
9. Xiao HD, Fuchs S, Campbell DJ, et al. Mice with cardiac-restricted angiotensin-converting enzyme (ACE) have atrial enlargement, cardiac arrhythmia, and sudden death. *Am J Pathol*. 2004; 165(3): 1019–32. [PubMed: 15331425]
10. Kasi VS, Xiao HD, Shang LL, et al. Cardiac-restricted angiotensin-converting enzyme overexpression causes conduction defects and connexin dysregulation. *Am J Physiol Heart Circ Physiol*. 2007; 293(1):H182–H192. [PubMed: 17337599]
11. Irvanian S, Sovari AA, Lardin HA, et al. Inhibition of renin-angiotensin system (RAS) reduces ventricular tachycardia risk by altering connexin43. *J Mol Med*. 2011 In press.

12. Gutstein DE, Morley GE, Tamaddon H, et al. Conduction slowing and sudden arrhythmic death in mice with cardiac-restricted inactivation of connexin43. *Circ Res.* 2001; 88(3):333–9. [PubMed: 11179202]
13. Das J, Chen P, Norris D, et al. 2-aminothiazole as a novel kinase inhibitor template. Structure-activity relationship studies toward the discovery of N-(2-chloro-6-methylphenyl)-2-[[6-[4-(2-hydroxyethyl)-1-piperazinyl]-2-methyl-4-pyrimidinyl]amino]-1,3-thiazole-5-carboxamide (dasatinib, BMS-354825) as a potent pan-Src kinase inhibitor. *J Med Chem.* 2006; 49(23):6819–32. [PubMed: 17154512]
14. Hennequin LF, Allen J, Breed J, et al. N-(5-chloro-1,3-benzodioxol-4-yl)-7-[2-(4-methylpiperazin-1-yl)ethoxy]-5- (tetrahydro-2H-pyran-4-yloxy)quinazolin-4-amine, a novel, highly selective, orally available, dual-specific c-Src/Abl kinase inhibitor. *J Med Chem.* 2006; 49(22):6465–88. [PubMed: 17064066]
15. Pham NA, Magalhaes JM, Do T, et al. Activation of Src and Src-associated signaling pathways in relation to hypoxia in human cancer xenograft models. *Int J Cancer.* 2009; 124(2):280–6. [PubMed: 18924149]
16. Trevino JG, Summy JM, Lesslie DP, et al. Inhibition of SRC expression and activity inhibits tumor progression and metastasis of human pancreatic adenocarcinoma cells in an orthotopic nude mouse model. *Am J Pathol.* 2006; 168(3):962–72. [PubMed: 16507911]
17. Wojcik EJ, Sharifpoor S, Miller NA, et al. A novel activating function of c-Src and Stat3 on HGF transcription in mammary carcinoma cells. *Oncogene.* 2006; 25(19):2773–84. [PubMed: 16407846]
18. Kieken F, Mutsaers N, Dolmatova E, et al. Structural and molecular mechanisms of gap junction remodeling in epicardial border zone myocytes following myocardial infarction. *Circ Res.* 2009; 104(9):1103–12. [PubMed: 19342602]
19. Aikawa R, Komuro I, Yamazaki T, et al. Oxidative stress activates extracellular signal-regulated kinases through Src and Ras in cultured cardiac myocytes of neonatal rats. *J Clin Invest.* 1997; 100(7):1813–21. [PubMed: 9312182]
20. Haendeler J, Hoffmann J, Brandes RP, Zeiher AM, Dimmeler S. Hydrogen peroxide triggers nuclear export of telomerase reverse transcriptase via Src kinase family-dependent phosphorylation of tyrosine 707. *Mol Cell Biol.* 2003; 23(13):4598–610. [PubMed: 12808100]
21. Khadaroo RG, He R, Parodo J, et al. The role of the Src family of tyrosine kinases after oxidant-induced lung injury in vivo. *Surgery.* 2004; 136(2):483–8. [PubMed: 15300219]
22. Liu Y, Bishop A, Witucki L, et al. Structural basis for selective inhibition of Src family kinases by PP1. *Chem Biol.* 1999; 6(9):671–8. [PubMed: 10467133]
23. Amoui M, Draber P, Draberova L. Src family-selective tyrosine kinase inhibitor, PP1, inhibits both Fc epsilonRI- and Thy-1-mediated activation of rat basophilic leukemia cells. *Eur J Immunol.* 1997; 27(8):1881–6. [PubMed: 9295022]
24. Hanke JH, Gardner JP, Dow RL, et al. Discovery of a novel, potent, and Src family-selective tyrosine kinase inhibitor. Study of Lck- and FynT-dependent T cell activation. *J Biol Chem.* 1996; 271(2):695–701. [PubMed: 8557675]
25. Morita N, Sovari AA, Xie Y, et al. Increased susceptibility of aged hearts to ventricular fibrillation during oxidative stress. *Am J Physiol Heart Circ Physiol.* 2009; 297(5):H1594–H1605. [PubMed: 19767530]
26. Sovari AA, Vahdani N, Morita N, Roos K, Weiss JN, Karagueuzian HS. Oxidative Stress Promotes Ventricular Fibrillation at the Early Stages of Hypertension: Role of Ca²⁺/CaM Kinase-II. *Heart Rhythm.* 7(suppl.):PO3–92.
27. el-Fouly MH, Trosko JE, Chang CC. Scrape-loading and dye transfer. A rapid and simple technique to study gap junctional intercellular communication. *Exp Cell Res.* 1987; 168(2):422–30. [PubMed: 2433137]
28. Rubart M, Zipes DP. Mechanisms of sudden cardiac death. *J Clin Invest.* 2005; 115(9):2305–15. [PubMed: 16138184]
29. Reaume AG, de Sousa PA, Kulkarni S, et al. Cardiac malformation in neonatal mice lacking connexin43. *Science.* 1995; 267(5205):1831–4. [PubMed: 7892609]

30. Thomas SP, Kucera JP, Bircher-Lehmann L, Rudy Y, Saffitz JE, Kleber AG. Impulse propagation in synthetic strands of neonatal cardiac myocytes with genetically reduced levels of connexin43. *Circ Res.* 2003; 92(11):1209–16. [PubMed: 12730095]

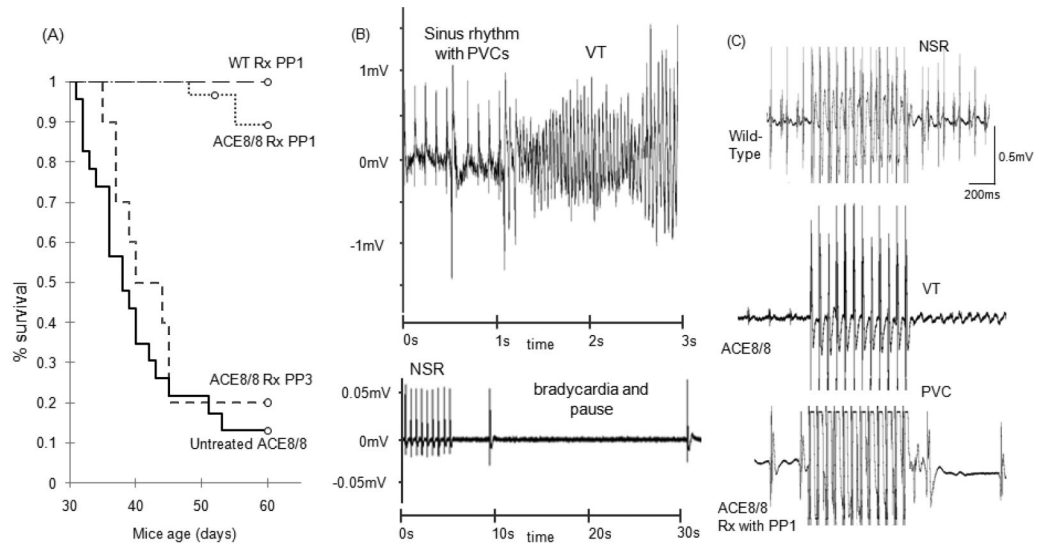


Figure 1. Survival analysis, telemetry monitoring and inducibility of VT

(A) Kaplan-Meier survival distribution analysis of ACE8/8 untreated mice, ACE8/8 mice that received PP3 treatment, ACE8/8 mice that received PP1 treatment, and wild-type mice that received PP1 treatment. PP1 treatment significantly reduced the sudden cardiac death rate with the mean survival time of 10.2 ± 1.5 days in ACE8/8 ($n=28$) and 24.7 ± 0.2 days in ACE8/8 treated with PP1 ($n=22$) ($P < 0.005$, log-rank test). No death happened in WT mice receiving PP1 treatment ($n=14$). PP3, the ineffective analog of PP1, did not increase the survival rate in ACE8/8 mice (11.2 ± 1.2 days vs. 10.2 ± 1.5 days, $P = \text{NS}$, $n=10$). (B) Examples of telemetry recording of the rhythm preceding SCD. The top panel shows an example of severe bradycardia and the bottom panel is an example of VT degenerating to VF resulting in SCD. The majority of SCD events resulted from ventricular arrhythmia (83%). (C) Inducibility of VT was tested using a 1.1F catheter and an internal jugular vein access. A rhythm with more than 3 consecutive ventricular beats was considered to be VT. Examples of intracardiac electrograms of WT, ACE8/8 and ACE8/8 treated with PP1 are shown after 12 beats of burst pacing with pacing cycle length of 50 ms. VT inducibility rate was statistically reduced with PP1 treatment in ACE8/8 mice (86.9% vs. 50%, $P < 0.05$, $n=20$ and $n=10$ respectively).

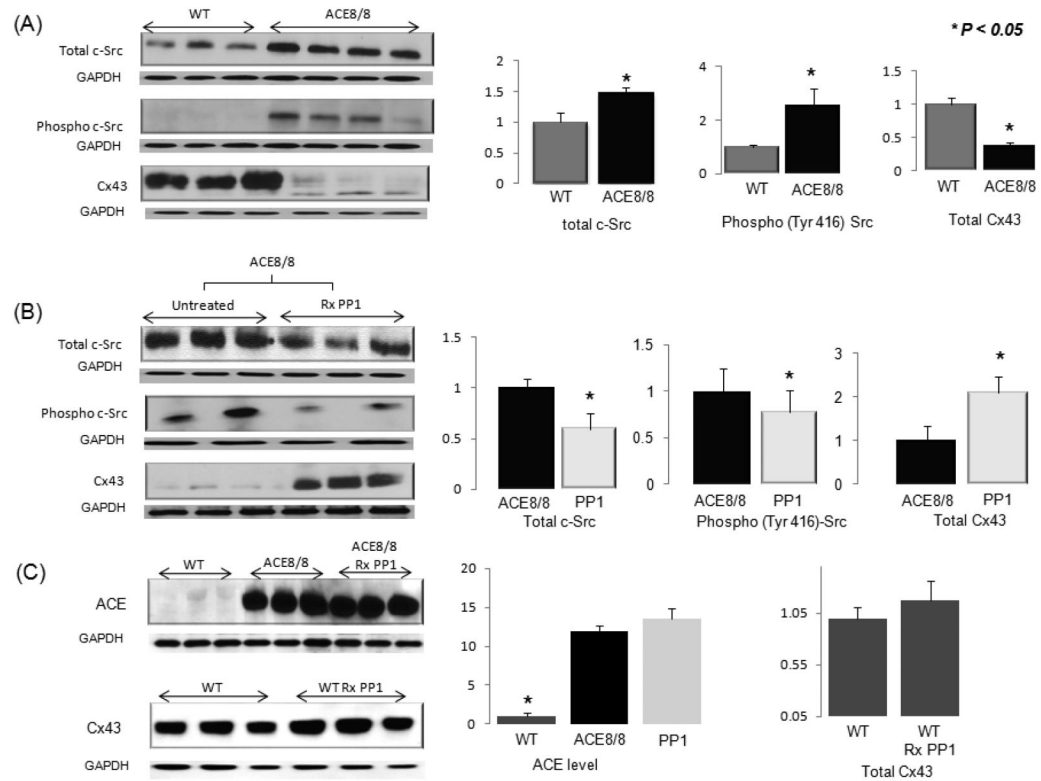


Figure 2. Western blot analysis of protein levels

All results are corrected for the GAPDH level. (A) The total c-Src protein level was 1.47-fold higher in ACE8/8 mice than in wild-type mice ($P < 0.05$), and the phospho-(Tyr416) c-Src protein level was 2.6-fold higher in ACE8/8 mice than in control mice ($P < 0.05$). The Cx43 level was reduced in ACE8/8 mouse hearts to 36% of the level in wild-type mouse hearts ($P < 0.005$ ($n=6$ for all groups)). (B) PP1 treatment: Four weeks of intraperitoneal injection of PP1 in ACE8/8 mice decreased the total c-Src protein level to 58% of that in untreated ACE8/8 mice ($P < 0.05$) and reduced the phospho-(Tyr 416) c-Src level to 75% of that in untreated ACE8/8 mice ($P < 0.05$). More importantly, PP1 treatment resulted in a 2.1-fold increase in the Cx43 level in ACE8/8 mice and increased the level of Cx43 to 68% of its normal level in wild-type mice ($n=6$ for all groups). (C) The ACE level was increased 11.9-fold in ACE8/8 mice compared to the control animals ($P < 0.005$). Treatment with PP1 did not change the cardiac ACE level in ACE8/8 mice ($P = NS$). Treatment of wild-type animals with PP1 did not change significantly the total level of Cx43 ($P = NS$) ($n=6$ for all groups).

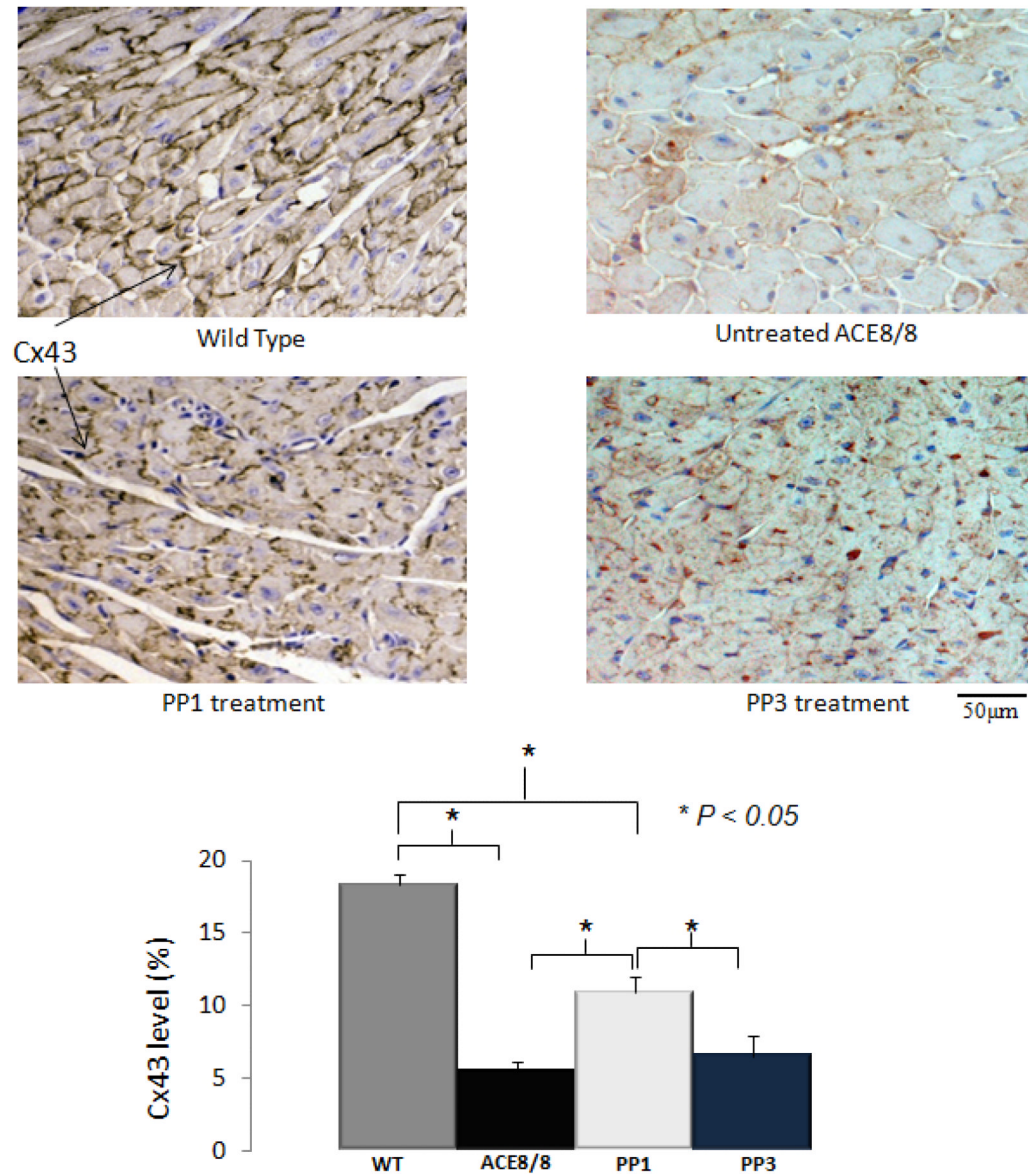


Figure 3. Results of immunostaining for Cx43

The Cx43 level which was measured as the ratio of stained area for Cx43 in the field of view to the total field of view was significantly lower in ACE8/8 mouse hearts than in wild-type mouse hearts ($18.3 \pm 0.6\%$ vs. $5.4 \pm 0.7\%$, $P < 0.005$). PP1 treatment resulted in a 2-fold increase in the Cx43 level in ACE8/8 mouse hearts ($P < 0.005$). The result of immunostaining for Cx43 was consistent with the result of western blotting and it confirmed that the improvement in the Cx43 protein level was associated with the increased level of this protein at its site of function, gap junctions. Treatment with PP3, the inactive analog of PP1, did not increase Cx43 level in compare to untreated ACE8/8 mice ($5.4 \pm 0.7\%$ vs. $6.5 \pm 0.7\%$, $P = \text{NS}$) ($n=4$ for all groups).

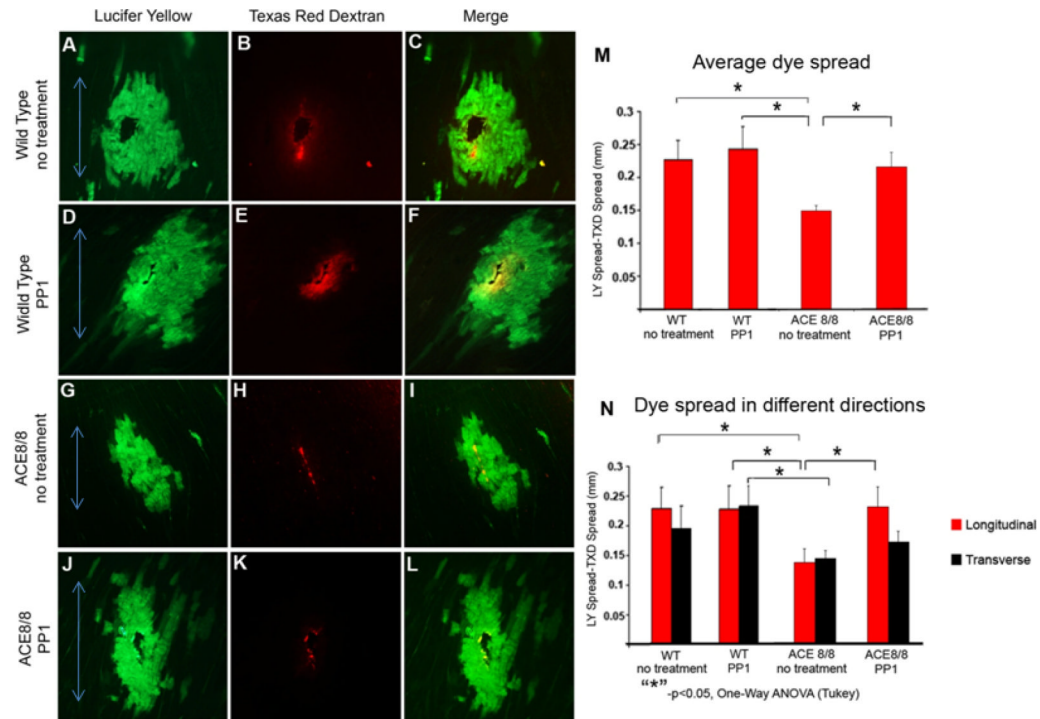


Figure 4.

Function of gap junctions was assessed by modified scrape loading. Lucifer Yellow (LY; 400kDa) spreads extensively through myocytes from WT hearts (A), far beyond the spread of TRD (B; 10000kDa). Overlay image is seen in C. In the ACE8/8 hearts LY spread is decreased (D) with fewer cells coupled beyond the TRD (E). Overlay image indicates that fewer cells are coupled in these ACE8/8 hearts (F). Treatment of mice with PP1 restores normal dye spread (G) to well beyond the TRD (H). Note that the overlay image from WT mice (C) and from the PP1 treated mice (I) are similar in the extent of dye spread seen. Quantification of the overall dye spread shows that the overall dye spread in the ACE8/8 mice is significantly decreased (0.14 ± 0.01 mm vs. 0.21 ± 0.02 mm respectively, $P < 0.05$) and that is restored to the normal level after PP1 treatment (0.21 ± 0.02 mm in WT vs. 0.20 ± 0.02 mm in PP1, $P = \text{NS}$, PP1 vs. ACE8/8 $P < 0.05$). Analysis of the anisotropy of dye spread indicates that in this model dye spread is lost in both the transverse and longitudinal directions, although more prominent in the longitudinal direction (K). Treatment of wild-type mice with PP1 did not significantly change the gap junction conduction ($P = \text{NS}$) ($n=5$ for all groups).

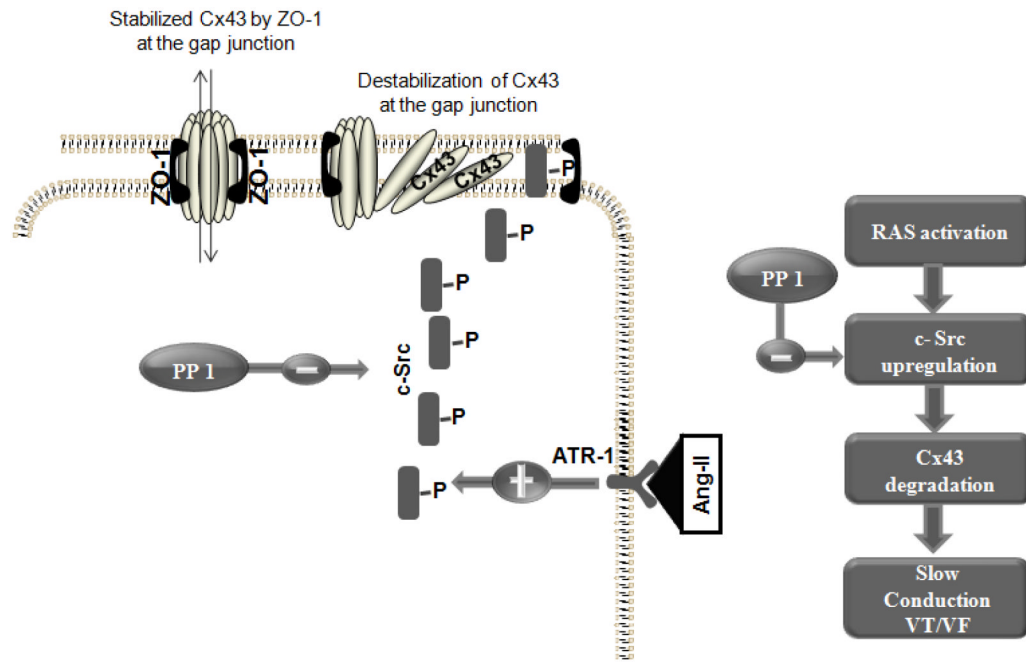


Figure 5. A schematic figure of the relation between Ang II, c-Src and Cx43
 c-Src mediates the effect of Ang II on Cx43 reduction and impaired gap junction function. PP1 is a known specific inhibitor of c-Src tyrosine kinase that interrupts Ang II mediated Cx43 reduction, myocyte uncoupling and sudden arrhythmic death.